INTERNATIONAL JOURNAL FOR NUMERICAL METHODS IN ENGINEERING
Int. J. Numer. Meth. Engng (2012)
Published online in Wiley Online Library (wileyonlinelibrary.com). DOI: 10.1002/nme.4367

A fast method for binary programming using first-order derivatives, with application to topology optimization with buckling constraints

P. A. Browne[1,*,†], C. Budd[1], N. I. M. Gould[2], H. A. Kim[3] and J. A. Scott[2]

[1]*Department of Mathematical Sciences, University of Bath, Bath, BA2 7AY, UK*
[2]*Numerical Analysis Group, STFC Rutherford Appleton Laboratory, Oxfordshire, OX11 0QX, UK*
[3]*Department of Mechanical Engineering, University of Bath, Bath, BA2 7AY, UK*

SUMMARY

We present a method for finding solutions of large-scale binary programming problems where the calculation of derivatives is very expensive. We then apply this method to a topology optimization problem of weight minimization subject to compliance and buckling constraints. We derive an analytic expression for the derivative of the stress stiffness matrix with respect to the density of an element in the finite-element setting. Results are presented for a number of two-dimensional test problems. Copyright © 2012 John Wiley & Sons, Ltd.

Received 17 November 2011; Revised 1 May 2012; Accepted 9 May 2012

KEY WORDS: topology optimization; buckling; eigenvalue; structural optimization; binary programming

1. INTRODUCTION

The problem considered in this paper is how to minimize the weight of an elastic structure whilst maintaining the integrity of the structure by prescribing two constraints. The first ensures that the structure has a prescribed level of stiffness, and the second that the structure is not prone to buckling. The purpose of this paper is to present an algorithm that can provide a solution for problems such as these in a reasonable computing time.

To formulate the problem mathematically, the design space (region in which material is placed) is discretized using finite elements. The goal of optimization is to determine which elements should contain material and which should be void of material. This is usually represented by a binary variable where a value of 1 is assigned to an element with material and a value of 0 to an element containing no material, thus resulting in a binary programming problem.

Finding a global solution to binary programming problems is notoriously difficult. The methods for finding such minima can be broadly put into three categories: implicit enumeration, branch-and-bound and cutting-plane methods. The most popular implementations involve hybrids of branch-and-bound and cutting-plane methods. For a comprehensive description of these binary programming methods, see, for example, Wolsey [1]. These methods were popular for structural optimization from the late 1960s through the early 1990s. In 1994, Arora and Huang [2] reviewed the methods for solving structural optimization problems discretely.

In 1968, Toakley [3] applied a combination of cutting-plane methods and branch-and-bound to solve truss optimization problems. Using what is now known as the branch-and-cut method,

*Correspondence to: P. A. Browne, Department of Mathematical Sciences, University of Bath, Bath, BA2 7AY, U.K.
†E-mail: P.A.Browne@bath.ac.uk

this method was resurged in 2010 by Stolpe and Bendsøe [4] to find the global solution to a minimization of compliance problem, subject to a constraint on the volume of the structure.

In 1980, Farkas and Szabo [5] applied an implicit enumeration technique to the design of beams and frames. Branch-and-bound methods have been used by, amongst others, John *et al*. [6], Sandgren [7, 8] and Salajegheh and Vanderplaats [9] for structural optimization problems. In the latest of these papers, the number of variables in the considered problem was 100 and in some cases took over 1 week of CPU time on a modern server to compute the solution. Whilst these methods do find global minima, they suffer from exponential growth in the computation time as the number of variables increases.

Beckers [10] used a dual method to find discrete solutions to structural optimization problems. In 2003, Stolpe and Svanberg [11] formulated a topology optimization problem as a mixed 0–1 programme and solved it using branch-and-bound methods.

Achtizger and Stolpe [12–14] have studied in detail the topology optimization of truss structures using branch-and-bound methods, and have been able to find global solutions to problems with over 700 bars in the ground structure.

To avoid the computational issues associated with binary programming, the traditional approach to topology optimization has been to relax the binary constraint and to look for a solution that varies continuously in $\mathbb{R}^n$. This is known as continuous relaxation of the problem. Physically, this relaxed variable can correspond to the stiffness of the material in the element. Nested analysis and design is then performed, meaning that the structural analysis of the current structure is carried out and appropriate derivatives calculated. These values are then fed to an optimization routine that updates the structure. The analysis is performed again and this process iterates until an optimum is attained.

By far, the most popular optimization method to update the structure is the Method of Moving Asymptotes (MMA) [15]. MMA requires the function values and values of the derivatives at the current iteration in order to progress to a new iteration with lower objective function. There are many examples of MMA being very efficient at solving topology optimization problems with different objectives/constraints (e.g. [16]). The buckling load of a structure is found as the solution to an eigenvalue problem, and a structure is said to buckle at the lowest positive eigenvalue, referred to as the critical load. Derivatives of this critical load are only well defined if there is a single modeshape corresponding to the critical load, that is, we have a simple eigenvalue. Hence, a direct bound on the critical load that cannot be used as a constraint with MMA as the derivative is not well defined.

Semidefinite programming methods have been developed specifically to deal with such eventualities. Kocvara [17], and in conjunction with Stingl [18], has applied such methods to topology optimization problems. More recently, along with Bogani [19], they have applied an adapted version of their semidefinite codes to find non-integer solutions to buckling problems. This made use of a reformulation of a semidefinite constraint using the indefinite Cholesky factorization of the matrix, and solving a resulting nonlinear programming problem with an adapted version of MMA. With these techniques, they were able to solve a non-discrete problem with 5000 variables in about 35 min on a standard PC.

When a continuous relaxation approach is used in problems involving calculating the buckling modes (or harmonic modes) of a structure, unwanted numerical effects are introduced. Tenek and Hagiwara [20], Pedersen [21] and Neves *et al*. [22] all noted that spurious buckling (or harmonic) modes would be computed in which the buckling is confined to regions where the density of material is less than 10%. Whilst assigning zero stress stiffness (or mass in the harmonic analysis case) contributions from these elements can eradicate these spurious modes; this is not consistent with the underlying model of the structure. Indeed, if one were to consider a structure where a small fraction (less than 10%) of material was equidistributed throughout the design domain, the stress stiffness matrix would be the zero matrix, and as a result, the critical load of the structure would be computed as infinite.

In this paper, we introduce an efficient method for binary programming and apply it to topology optimization problems with a buckling constraint. In doing so, we avoid the problem of spurious buckling modes and can find solutions to large two-dimensional problems ($\mathcal{O}(10^5)$ variables).

Because of the dimensionality of the problems, and the complexity of derivative-free methods for binary programmes, we will use derivative information to reduce this complexity. The efficiency of topology optimization methods involving a buckling constraint is severely hindered by the calculation of the derivatives of the buckling constraint. This calculation typically takes an order of magnitude more time than the linear elasticity analysis. With this in mind, the proposed fast binary descent method we introduce will try to reduce the number of derivative calculations required.

The remainder of this paper is organized as follows. In Section 2, we formulate the topology optimization problem to include a buckling constraint. Section 3 motivates and states the new method, which we use to solve the optimization problem. Section 4 then contains implementation details and results for a number of two-dimensional test problems. Finally in Section 5, we draw conclusions about the proposed algorithm.

2. FORMULATION OF TOPOLOGY OPTIMIZATION TO INCLUDE A BUCKLING CONSTRAINT

Let Ω be the design domain containing the elastic structure that is discretized using a finite-element mesh $\mathcal{T}$. A load f is applied to Ω, and this induces displacements u, which are the solution to the equilibrium equations of linear elasticity

$$Ku = f \tag{1}$$

where K is the finite-element stiffness matrix. Compliance, defined as the product $f^T u$, is a measure of external work done on the structure and adding an upper bound $c_{\max}$ ensures that the structure remains stiff.

The minimization of weight subject to a compliance constraint is a well-studied problem, for example, [16]. However, it has long been observed that structures optimized for minimum weight or compliance are prone to buckling [23].

The critical buckling load of a structure is defined by the smallest positive value of λ corresponding to a nonzero v for which

$$(K + \lambda K_\sigma)v = 0. \tag{2}$$

In this equation, K is the symmetric finite-element stiffness matrix, and K_σ is the symmetric stress stiffness matrix. (λ, v) is an eigenpair of the generalized eigenvalue problem (2). λ is referred to as the eigenvalue and $v \neq 0$ the corresponding eigenvector (or mode shape). The critical load is λ times the applied load f. Given a safety factor parameter $c_s > 0$, a bound of the form $\lambda \geqslant c_s$ is equivalent to the semidefinite constraint

$$K + c_s K_\sigma \succeq 0.$$

This means that all the eigenvalues of the system $(K + c_s K_\sigma)$ are non-negative. This happens only if $\sum_{i=1}^{M} v_i^T (K + c_s K_\sigma) v_i \geqslant 0$ where v_i are the M buckling modes that solve $(K + \lambda K_\sigma)v_i = 0$. If we let $x \in \{0,1\}^n$ represent the density of material in each of the elements of the mesh, with $x_i = 0$ corresponding to an absence of material in element i and $x_j = 1$ corresponding to element j being filled with material, the problem to be solved becomes

$$\min_x \sum x_j \tag{3a}$$

$$\text{subject to} \qquad c_1(x) := c_{\max} - f^T u(x) \geqslant 0 \tag{3b}$$

$$c_2(x) := \sum_{i=1}^{M} v_i(x)^T (K(x) + c_s K_\sigma(x)) v_i(x) \geqslant 0 \tag{3c}$$

$$x \in \{0,1\}^n \tag{3d}$$

$$K(x)u(x) = f \tag{3e}$$

$$[K(x) + \lambda(x) K_\sigma(x)] v_i(x) = 0. \quad \forall i = 1, \ldots, M \tag{3f}$$

2.1. Derivative calculations

To use the binary descent method (discussed in Section 3) we need an efficient way of calculating the derivative of the constraints with respect to the variables x_i. As will be seen in Section 4, the computation of derivatives of the buckling constraint (3c) is the bottleneck in our optimization algorithm, so it is imperative that we have an analytic expression for this. To calculate the derivatives, the binary constraints on the variables are relaxed and assume that the following holds

$$K(x) = \sum_{\ell} x_\ell K_\ell,$$

where K_ℓ is the local element stiffness matrix. The derivative of this with respect to the density of an element x_i is given by

$$\frac{\partial K}{\partial x_i}(x) = K_i.$$

Calculating the derivative of the buckling constraint requires the derivation of an expression for $\frac{\partial K_\sigma}{\partial x_i}$. This quantity is nontrivial to compute, unlike the derivative of a mass matrix, which would be in place of the stress stiffness matrix in structural optimization involving harmonic modes. The stress field σ_ℓ on an element ℓ is a 3×3 tensor with six DOFs. This can be written in three dimensions as follows:

$$\sigma_\ell = \begin{bmatrix} \sigma_{11} \\ \sigma_{22} \\ \sigma_{33} \\ \sigma_{12} \\ \sigma_{13} \\ \sigma_{23} \end{bmatrix}_\ell = x_\ell E_\ell B_\ell u,$$

which in two dimensions reduces to

$$\sigma_\ell = \begin{bmatrix} \sigma_{11} \\ \sigma_{22} \\ \sigma_{12} \end{bmatrix}_\ell = x_\ell E_\ell B_\ell u,$$

where u are the nodal displacements of the element, E_ℓ is a constant matrix of material properties and B_ℓ contains geometric information about the element. The indices $1, 2$ and 3 refer to the coordinate directions of the system.

We consider the two-dimensional case and note that all the following steps have a direct analogue in three dimensions. We write the stress stiffness matrix given in (2) as follows.

$$K_\sigma = \sum_{\ell=1}^{n} \int G_\ell^T \begin{bmatrix} \sigma_{11} & \sigma_{12} & 0 & 0 \\ \sigma_{12} & \sigma_{22} & 0 & 0 \\ 0 & 0 & \sigma_{11} & \sigma_{12} \\ 0 & 0 & \sigma_{12} & \sigma_{22} \end{bmatrix}_\ell G_\ell \mathrm{d}V_\ell, \tag{4}$$

where G_ℓ is a matrix containing derivatives of the basis functions that relates the displacements of an element ℓ to the nodal DOFs [24], and n is the total number of elements in the finite-element mesh $\mathcal{T}$. Now, define a map $\Theta : \mathbb{R}^3 \mapsto \mathbb{R}^{4\times4}$ by

$$\Theta\left(\begin{bmatrix} \alpha \\ \beta \\ \gamma \end{bmatrix}\right) := \begin{bmatrix} \alpha & \gamma & 0 & 0 \\ \gamma & \beta & 0 & 0 \\ 0 & 0 & \alpha & \gamma \\ 0 & 0 & \gamma & \beta \end{bmatrix}.$$

Note that Θ is a linear operator. Using this, (4) becomes

$$\begin{aligned} K_\sigma &= \sum_{\ell=1}^{n} \int G_\ell^T \, \Theta(x_\ell E_\ell B_\ell u) G_\ell \, \mathrm{d}V_\ell \\ &= \sum_{\ell=1}^{n} \int G_\ell(\boldsymbol{\xi})^T \, \Theta(x_\ell E_\ell B_\ell(\boldsymbol{\xi}) u) G_\ell(\boldsymbol{\xi}) \, \mathrm{d}V_\ell \\ &\approx \sum_{\ell=1}^{n} \sum_{j} \omega_j G_\ell(\boldsymbol{\xi}_j)^T \, \Theta(x_\ell E_\ell B_\ell(\boldsymbol{\xi}_j) u) G_\ell(\boldsymbol{\xi}_j) \end{aligned} \tag{5}$$

where ω_j are the weights associated with the appropriate Gauss points $\boldsymbol{\xi}_j$ that implement a chosen quadrature rule to approximate the integral. Differentiating the equilibrium equation (1) with respect to the density x_i yields

$$\frac{\partial K}{\partial x_i} u + K \frac{\partial u}{\partial x_i} = 0$$

and hence

$$\frac{\partial u}{\partial x_i} = -K^{-1} \frac{\partial K}{\partial x_i} u.$$

Now consider the derivative of the operator Θ with respect to x_i. Since Θ is linear

$$\begin{aligned} \frac{\partial \Theta(x_\ell E_\ell B_\ell u)}{\partial x_i} &= \Theta\left(\frac{\partial}{\partial x_i} x_\ell E_\ell B_\ell u(x_i) \right) \\ &= \Theta\left(\delta_{i\ell} E_\ell B_\ell(\xi_j) u + x_\ell E_\ell B_\ell(\xi_j) \frac{\partial u}{\partial x_i} \right) \end{aligned}$$

where $\delta_{i\ell}$ is the Kronecker Delta.

Applying the chain rule to (5), we obtain

$$\begin{aligned} \frac{\partial K_{\boldsymbol{\sigma}}}{\partial x_i} &\approx \sum_{l=1}^{n} \sum_{j} \omega_j G_\ell(\boldsymbol{\xi}_j)^T \frac{\partial \Theta(x_\ell E_\ell B_\ell(\boldsymbol{\xi}_j) u)}{\partial x_i} G_\ell(\boldsymbol{\xi}_j) \\ \frac{\partial K_{\boldsymbol{\sigma}}}{\partial x_i} &\approx \sum_{l=1}^{n} \sum_{j} \omega_j G_\ell(\boldsymbol{\xi}_j)^T \, \Theta\left(\delta_{i\ell} E_\ell B_\ell(\boldsymbol{\xi}_j) u - x_\ell E_\ell B_\ell(\boldsymbol{\xi}_j) K^{-1} \frac{\partial K}{\partial x_i} u \right) G_\ell(\boldsymbol{\xi}_j), \end{aligned} \tag{6}$$

where the approximation is due to the error in the quadrature rule used. This matrix can now be used to find the derivative of the buckling constraint that we require. For each variable $x_i = 1, \dots, n$, (6) must be computed. As (6) contains a sum over $i = 1, \dots, n$, it can be seen that computing $\frac{\partial K_\sigma}{\partial x_i}$ has computational complexity of $\mathcal{O}(n)$ for each i and hence computing (6) for all variables has complexity of $\mathcal{O}(n^2)$.

3. FAST BINARY DESCENT METHOD

In this section, we motivate and describe the new method that we propose for solving the binary programming problem. If we solve the state equations (3e) and (3f), then problem (3) takes the general form

$$\min_x e^T x \tag{7a}$$

$$\text{subject to} \quad c(x) \geqslant 0 \tag{7b}$$

$$x \in \{0, 1\} \tag{7c}$$

with $x \in \mathbb{R}^n$, $c \in \mathbb{R}^m$ and $e = [1, 1, \dots, 1]^T \in \mathbb{R}^n$ and note that problem (3) is of this form. Typically m will be small (less than 10) and $m << n$. We also assume that $x^0 = e$ is an initial feasible point of (7). Let k denote the current iteration, and x^k is the value of x on the kth iteration.

The objective function $e^T x$ is a linear function of x that can be optimized by successively reducing the number of nonzero terms in x, and we need not worry about errors in approximating this. However, the constraints are nonlinear functions of x and ensuring that (7b) holds is difficult. Accordingly, we now describe how a careful linearization of the constraint equations can lead to a feasible algorithm. Taylor's theorem can be used to approximate $c(x^k)$

$$c\left(x^{k+1}\right) = c(x^k) + \sum_{i=1}^{n} \frac{\partial c(x^k)}{\partial x_i}\left(x_i^{k+1} - x_i^k\right) + \text{ higher-order terms}$$

where $\frac{\partial c(x^k)}{\partial x_i}$ is determined using the explicit derivative results of the previous section. The method will take discrete steps so that

$$x_i^{k+1} - x_i^k \in \{-1, 0, 1\} \qquad \forall i = 1, \dots, n,$$

and so we must assume that the higher-order terms will be small, but later, a strategy will be introduced to cope with this when they are not.

Consider now variables x_i^k such that $x_i^k = 1$ that we wish to change to $x_i^{k+1} = 0$. Because $x_i^{k+1} - x_i^k = -1$, for the difference in the linearized constraint functions

$$c\left(x^{k+1}\right) - c(x^k) = \sum_{i=1}^{n} \frac{\partial c(x^k)}{\partial x_i}\left(x_i^{k+1} - x_i^k\right)$$

to be minimal, all the terms of $\frac{\partial c(x^k)}{\partial x_i}$ need to be as small as possible. However, because there are multiple constraints, the variables for which the gradient of one constraint is small may have a large gradient for another constraint.

Assuming a feasible point such that $c(x^k) > 0$ and ignoring the higher order terms,

$$c\left(x^{k+1}\right) = c(x^k) + \sum_{i=1}^{n} \frac{\partial c(x^k)}{\partial x_i}\left(x_i^{k+1} - x_i^k\right). \tag{8}$$

We have to ensure $c\left(x^{k+1}\right) > 0$, so

$$c(x^k) + \sum_{i=1}^{n} \frac{\partial c(x^k)}{\partial x_i}\left(x_i^{k+1} - x_i^k\right) > 0$$

or equivalently

$$1 + \sum_{i=1}^{n} \frac{\partial c_j^T(x^k)}{\partial x_i} / c_j(x^k)\left(x_i^{k+1} - x_i^k\right) > 0 \qquad \forall j = 1, \dots, m.$$

If $x_i^{k+1} \neq x_i^k$ then each normalized constraint $c_j(x^k)$ is changed by $\pm \frac{\partial c_j(x^k)}{\partial x_i} / c_j(x^k)$.

Define the sensitivity of variable i to be

$$s_i(x^k) = \max_{j=1,\dots,m} \frac{\partial c_j(x^k)}{\partial x_i} / \max\left\{c_j(x^k), 10\epsilon\right\} \tag{9}$$

where ϵ is the machine epsilon that guards against round off errors. For each variable, $s_i(x^k)$ is the most conservative estimate of how the constraints will vary if the value of the variable is changed. In one variable, this has the form shown in Figure 1. Figure 1(a) shows the absolute values of the linear approximations to the constraints based on their values and corresponding derivatives. Figure 1(b)

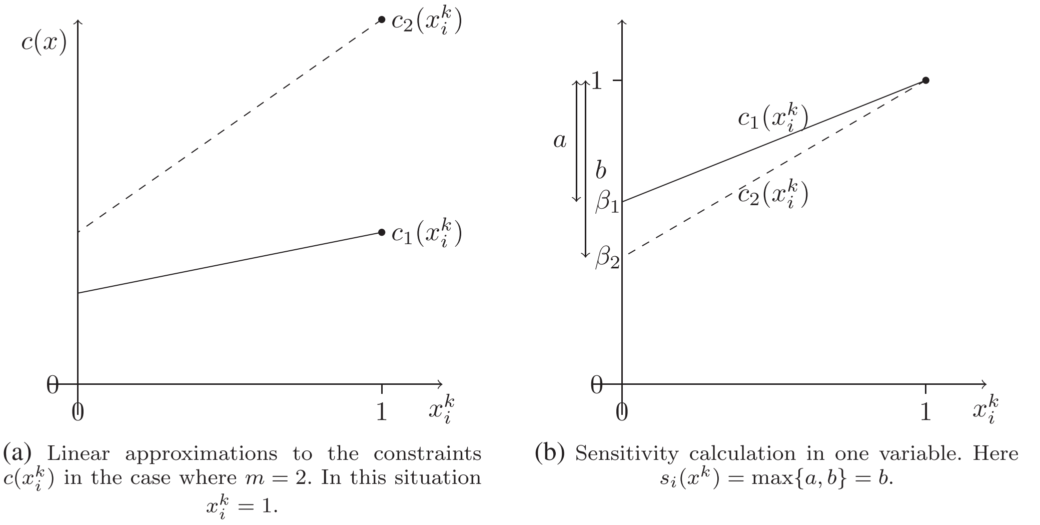

Figure 1. Sensitivity calculation in one variable for the case when $m = 2$. (a) Linear approximations to the constraints $c\left(x_i^k\right)$ in the case where m = 2. In this situation $x_i^k = 1$. (b) Sensitivity calculation in one variable. Here, $s_i(x^k) = \max\{a, b\} = b$.

shows the calculation that we make based on normalizing these approximations to compute which of the constraints would decrease the most if the variable x_i^k were changed. β_j is the point at which the line associated with the constraint c_j crosses the y-axis and so $\beta_j = 1 - \frac{\partial c_j(x^k)}{\partial x_i}/c_j(x^k)$. The amount that the normalized constraint c_j would change if the variable x_i^k were changed is then given by $1 - \beta_j = \frac{\partial c_j(x^k)}{\partial x_i}/c_j(x^k)$.

In this case, the derivatives indicate that if the variable x_i^k were to be decreased, the second constraint is affected relatively more than the first constraint (as $\max\{a, b\} = b$), and hence, the sensitivity associated with this variable x_i is given the value $s_i(x^k) = \frac{\partial c_2(x^k)}{\partial x_i}/c_2(x^k)$.

This sensitivity measure also provides an ordering so that if we choose to update variables in increasing order of their sensitivity, the changes in the constraint values are minimized. Now, for ease of notation, let us assume that the variables are ordered so that

$$s_1 \leqslant s_2 \leqslant \ldots \leqslant s_p \qquad \forall s_i \text{ s.t. } x_1^k, x_2^k, \ldots, x_p^k = 1 \tag{10}$$

$$s_{p+1} \geqslant s_{p+2} \geqslant \ldots \geqslant s_n \qquad \forall s_i \text{ s.t. } x_n^k, x_{n-1}^k, \ldots, x_{p+1}^k = 0 \tag{11}$$

To be cautious, instead of requiring $c(x^{k+1}) \geqslant 0$, we allow for the effects of the nonlinear terms and so are content if instead $c(x^{k+1}) \geqslant (1-\alpha)c(x^k)$ for some $\alpha \in (0, 1)$. This implies that

$$c(x^k) + \sum_{i=1}^{n} \frac{\partial c^T(x^k)}{\partial x_i}\left(x_i^{k+1} - x_i^k\right) \geqslant (1-\alpha)c(x^k),$$

or equivalently

$$\alpha c(x^k) + \sum_{i=1}^{n} \frac{\partial c^T(x^k)}{\partial x_i}\left(x_i^{k+1} - x_i^k\right) \geqslant 0.$$

To update the current solution, we consider the variables ordered so that (10) and (11) hold and find for some $\alpha \geqslant 0$

$$L := \max_{1 \leqslant \ell \leqslant p} \ell \quad \text{s.t.} \quad \alpha c_j(x^k) - \sum_{i=1}^{\ell} \frac{\partial c_j(x^k)}{\partial x_i} > 0 \qquad \text{for all} \quad j \in 1, \ldots, m. \tag{12}$$

Then we decrease from 1 to 0 those variables $x_1^k, \dots, x_L^k$ so as to reduce the objective function by a value of L.

However, there is the possibility that increasing variables from 0 to 1 could further reduce the objective function by reducing yet more variables from 1 to 0. This is tested by finding (or attempting to find) $J > 0$ such that

$$J := \max_{0 \leqslant \ell \leqslant (p-L)/2} \ell \quad \text{s.t.} \quad \sum_{i=1}^{\ell} \frac{\partial c_j(x^k)}{\partial x_{p+i}} - \sum_{i=1}^{2\ell} \frac{\partial c_j(x^k)}{\partial x_{L+i}} \geqslant 0 \qquad \text{for all } \; j \in 1, \dots, m. \tag{13}$$

So, the variables corresponding to the terms in the first sum are increased from 0 to 1, but for each of these two variables are decreased from 1 to 0, corresponding to the terms in the second summation. As there are more terms in the second summation, the objective function improves whilst remaining a feasible solution. Hence, the variables $x_{L+1}^k, \dots, x_{L+2J}^k$ are decreased from 1 to 0, and the variables $x_{p+1}^k, \dots, x_{p+J}^k$ are increased from 0 to 1. Note that in (12) and (13) the equations have to hold for each of the constraints $j = 1, \dots, m$.

The coefficient α is a measure of how well the linear gradient information is predicting the change in the constraints. If the problem becomes infeasible, then the method has taken too large a step, so α is reduced in order to take a smaller step. However, recall that the goal of this method is to compute the gradients as few times as possible, and so we wish to take steps that are as large as possible. If the step has been accepted for the previous two iterations without reducing α then α is increased to try and take larger steps and thus speed up the algorithm.

Note that if α is too large and the solution becomes infeasible, then α is reduced and a smaller step is taken without recomputing the derivatives. Hence, increasing α by too much is not too detrimental to the performance of the algorithm. Based on experience, α is reset to 0.7α when the solution becomes infeasible and α is set to 1.5α when we want to increase it. These values appear stable and give good performance for most problems.

To ensure that at least one variable is updated, α must be larger than a critical value α_c given by

$$\alpha_c = \max_{j=1,\dots,m} \left\{ \left(\frac{\partial c_j(x^k)}{\partial x_1^k} \right) / c_j(x^k) \right\}.$$

This guarantees that $L \geqslant 1$ and at least one variable is updated. The upper bound $\alpha \leqslant 1$ must also be enforced so that $c(x^{k+1}) \geqslant 0$.

If we cannot make any further progress with this algorithm, we stop. Making further progress would be far too expensive as we would have to switch to a different integer programming strategy, and the curse of dimensionality for the problems that we wish to consider prohibits this. However, we believe the computed solution is good because if we try and improve the objective function by changing the variable for which the constraints are infinitesimally least sensitive, the solution becomes infeasible.

The fast binary descent algorithm is thus presented in Algorithm 1.

4. IMPLEMENTATION AND RESULTS

We consider optimizing isotropic structures with Young's modulus 1.0 and Poisson's ratio 0.3. The design spaces are discretized using square bilinear elements on a uniform mesh.

The fast binary descent method has been implemented in Fortran90 using the HSL mathematical software library [25] and applied to a series of two-dimensional structural problems. The linear solve for the calculation of displacements (1) used HSL_MA87 [26], a DAG based direct solver designed for shared memory systems. For the size of problems considered, HSL_MA87 has been found to be very efficient and stable. The first six buckling modes of the system (2) were computed as these were sufficient to ensure all corresponding eigenvectors of the critical load were found. These eigenpairs were calculated using HSL_EA19 [27], a subspace iteration code, preconditioned by the Cholesky factorization already computed by HSL_MA87. The sensitivities were passed through a

Algorithm 1 Fast binary descent method

```
1: Initialise $x^0$ and $\alpha$.
2: Compute objective function (7a) and constraints (7b)
3: if $x^0$ not feasible then
4:     Stop
5: else
6:     Compute derivatives $\frac{\partial c(x^k)}{\partial x_i}$
7:     Sort $s_i$ (9)
8:     Compute values $L$ from (12) and $J$ from (13)
9:     Update the variables $x_i^k$ that correspond to $L$ and $J$ from (12) and (13)
10:    if no variables updated then
11:        {Algorithm has converged}
12:        return with computed solution
13:    end if
14:    Compute objective function and constraints from equations (7a) and (7b).
15:    if not feasible then
16:        {Reject update step}
17:        Reduce $\alpha$.
18:        GO TO 8
19:    else
20:        {Accept update step}
21:        Increase $\alpha$ if desired
22:        $k = k + 1$
23:        GO TO 6
24:    end if
25: end if
```

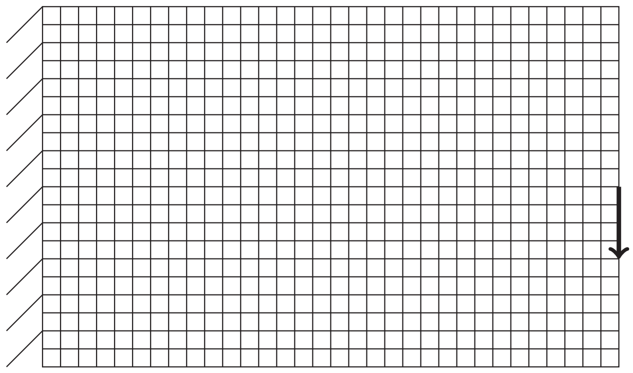

Figure 2. Design domain of a centrally loaded cantilevered beam. The aspect ratio of the design space is 1.6, and a unit load is applied vertically from the centre of the right hand side of the domain.

standard low-pass filter [28] with radius 2.5h where h is the width of an element and ordered using HSL_KB22, a heapsort [29] algorithm.

The codes were executed on a desktop with an Intel® Core™2 Duo CPU E8300 @ 2.83 Ghz with 2 GB RAM running a 32-bit Linux OS and were compiled with the gfortran compiler in double precision. All reported times are wall-clock times measured using `system_clock`.

4.1. *Short cantilevered beam*

We consider a clamped beam with a vertical unit external force applied to the free side as shown in Figure 2. Figures 3–5 refer to the solutions found with the same design domain and material properties, but with buckling and compliance constraints.

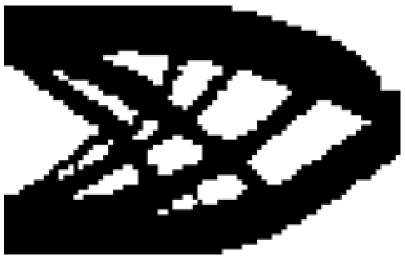
Figure 3. Solution found on mesh of 80 × 50 elements. The buckling constraint is set to $c_s = 0.9$ and the compliance constraint $c_{\max} = 35$. A volume of 0.6255 is attained. The buckling constraint c_2 is active, and the compliance constraint c_1 is not.

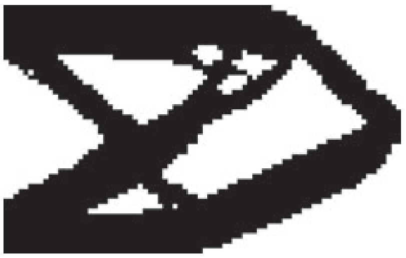
Figure 4. Solution found on mesh of 80 × 50 elements. The buckling constraint is set to $c_s = 0.9$ and the compliance constraint $c_{\max} = 60$. A volume of 0.5535 is attained. Here, the buckling constraint c_2 is active, and the compliance constraint c_1 is not.

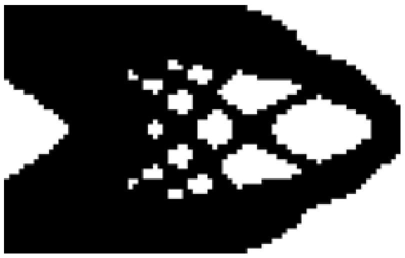
Figure 5. Solution found on mesh of 80 × 50 elements. The buckling constraint is set to $c_s = 0.1$ and the compliance constraint $c_{\max} = 30$. A volume of 0.692 is attained. Here, the compliance constraint c_1 is active, and the buckling constraint c_2 is not.

Figure 3 is the computed solution to the problem with parameters $c_s = 0.9$ in (3c) and $c_{\max} = 35$ in (3b). In this case, the compliance constraint $c_1(x^0)$ is large initially but the buckling constraint $c_2(x^0)$ is small initially. We see that the method has produced a typical optimum grillage structure with four bars under compression and only three bars under tension. Note that in the upper bar near the point of loading, there is a distinct corner in the computed solution. This type of formation attracts high concentrations of strain energy, and so, if the problem were minimization of compliance, then an optimization method would wish to avoid such situations. However, in this case, optimization of this region is primarily dominated by the buckling constraint, and the compliance is not the critical constraint.

Figure 4 is the computed solution to a problem with the same buckling constraint as in Figure 3 ($c_s = 0.9$) but is allowed to be more flexible with $c_{\max} = 60$ (i.e., the compliance constraint is not as restrictive). This results in a clear asymmetry in the computed solution in which the lower bar is much thicker than the upper bar. This lower bar is under compression with this loading, and hence would be prone to buckling. Thus optimization reinforced the lower bar to meet the buckling constraint.

Figure 5 was obtained as the solution for a problem with $c_s = 0.1$ and $c_{\max} = 30$. In this case, the initial value of $c_1(x^0)$ is close to 0. The computed solution has only the compliance constraint active, and hence, the computed solution is more symmetrical than the solutions shown in Figures 3 and 4.

From Figures 3–5, it is possible to see a clear difference in the topology of the resulting solution depending on the parameters c_s and $c_{\max}$. Note that whilst one constraint may be violated if the updating process were to proceed, the other constraints have been utilized throughout the computation and have affected the path taken and resulting solution of the algorithm. The history of the algorithm when applied to the problem solved in Figure 3 where $c_{\max} = 35$ and $c_s = 0.9$ is displayed in Figures 6–8.

The plot of the objective function against iteration number shown in Figure 6 is monotonically decreasing and so shows that the method as described in Section 3 is indeed a descent method. Note that in the initial stages of the computation, large steps are made and this varies as the computation progresses. Until iteration 4 large steps have been made and thus the objective function is swiftly decreasing. When going to iteration 5 taking a large step would make the current solution infeasible so the method automatically decreases the step size and hence the decrease in the objective function is reduced.

Figure 7 shows that the compliance constraint is inactive at the solution of this problem. Note that at all points the compliance of the structure is below the maximum compliance $c_{\max}$, and so, the solution is feasible at all points with respect to c_1. If this plot is compared with Figure 6, then the large changes in compliance can be seen to occur where there are large reductions in volume and similarly when there is a small change in the volume, the change in compliance is also small.

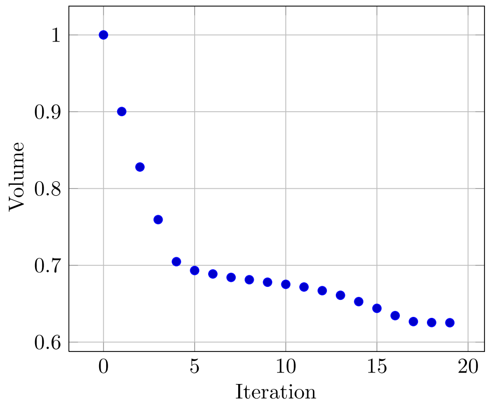

Figure 6. Volume–iterations of the fast binary descent method.

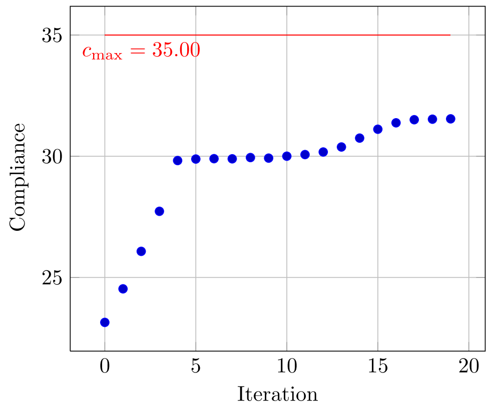

Figure 7. Compliance–iterations of the fast binary descent method.

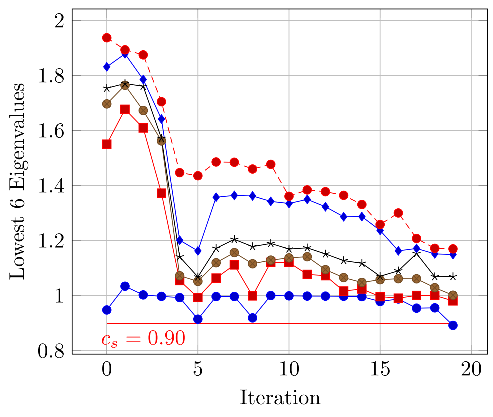

Figure 8. Eigenvalues–iterations of the fast binary descent method. Note that on the 20th iteration, the eigenvalue constraint is violated; thus, the computed solution is at the 19th iteration.

Figure 8 shows the lowest six eigenvalues of the system as the binary descent method progresses. We see that on the 20th iteration, the lowest eigenvalue is below the constraint c_s, and so, the computed solution is at iteration 19. At iterations 5 and 8 we see that the eigenvalue constraint is close to being violated. The increase in the lowest eigenvalue at the subsequent steps corresponds to a local thickening of the structure around the place where the buckling is most concentrated. This shows that the method has re-introduced material in order to move away from the constraint boundary. The nonlinearity in $c_2(x)$ is clear from the non-monotonic behaviour seen in Figure 8. Generally, we do see the eigenvalues converging and that supports the intuitive optimality criteria of coincidental eigenvalues.

Figure 8, when viewed in combination with Figure 7 shows that for the history of the algorithm, the solutions are all feasible.

4.2. *Side loaded column*

In this section, we consider a tall design space fixed completely at the bottom carrying a vertical load applied at the top corner of the design space. The design space is shown in Figure 9(a), and the computed solutions to this problem with differing constraints are shown in Figures 9(b) and (c). The problem solved in Figure 9(b) has $c_s = 0.225$ and $c_{\max} = 22.5$. The problem solved in Figure 9(c) has $c_s = 0.001$ and $c_{\max} = 60$.

In Figure 9(c), as the constraints are relaxed compared with the problem in Figure 9(b), the computed solution has a significantly lower objective function. However, it follows the same structural configuration where the main compressive column directly under the load resists the buckling and the slender column on the side provides additional support in tension to reduce bending. In both of these structures the path of the optimization is driven by the first buckling mode.

4.3. *Centrally loaded column*

We consider a square design domain (Figure 10). A unit load is applied vertically downwards at the centre of the top of the design domain, and the base is fixed.

Figures 11–14 present results for a mesh of 60×60 elements for a range of values of the constraints. Figures 11 and 12 have $c_s = 0.5$ with $c_{\max} = 5$ and $c_{\max} = 5.5$, respectively. This small change in the compliance constraint results in two distinct configurations. Figure 12 with the higher compliance constraint achieves a lower volume and has the buckling constraint active as opposed to the compliance constraint which is active in Figure 11.

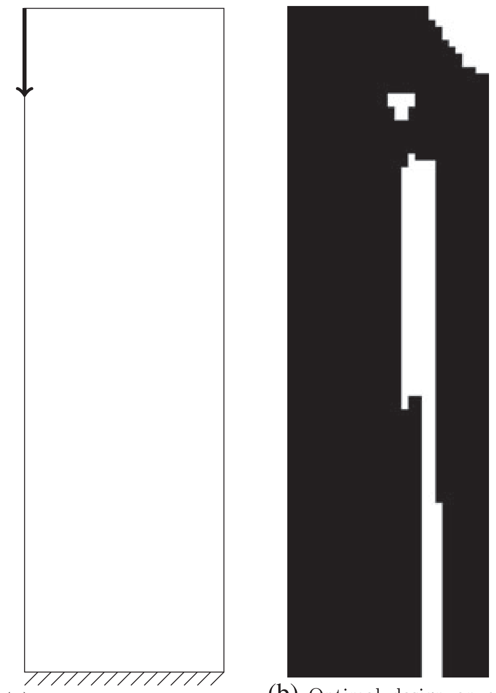

(a) Design domain with width to height ratio 3 : 10.

(b) Optimal design on a 30×100 mesh with $c_s = 0.225$ and $c_{\max} = 22.5$. Here c_2 is active and c_1 is not.

(c) Optimal design on a 30×100 mesh with $c_s = 0.001$ and $c_{\max} = 60$. Here c_1 is active and c_2 is not.

Figure 9. A column loaded at the side. (a) Design domain with width to height ratio 3 : 10. (b) Optimal design on a 30×100 mesh with $c_s = 0.225$ and $c_{\max} = 22.5$. Here, c_2 is active and c_1 is not. (c) Optimal design on a 30×100 mesh with $c_s = 0.001$ and $c_{\max} = 60$. Here, c_1 is active and c_2 is not.

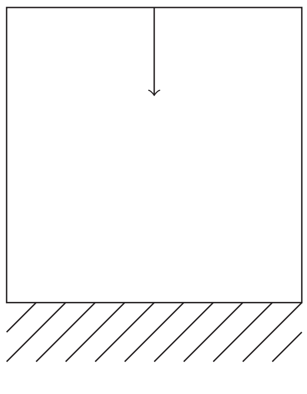

Figure 10. Design domain of model column problem. This is a square domain of side length 1 with a unit load acting vertically at the midpoint of the upper boundary of the space.

Distinct ‘Λ-*like*’ structures have been found in Figures 13 and 14. These problems share the parameter $c_{\max} = 8$, but vary in that they have $c_s = 0.4$ and $c_s = 0.1$, respectively. The higher buckling constraint of Figure 13 leads to the development of thick regions in the centre of the supporting legs. These regions help to resist the first-order buckling mode of the individual legs and are not seen in Figure 14 as the buckling constraint is lower. Figure 15 is the solution to a problem with the same parameters as the problem considered in Figure 14, but is solved on a much finer 200×200 mesh.

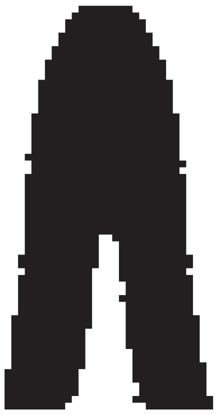

Figure 11. Solution computed on a mesh of 60×60 elements. The buckling constraint is set to $c_s = 0.5$ and the compliance constraint $c_{\max} = 5$. Here, the compliance constraint is active and the buckling constraint is inactive.

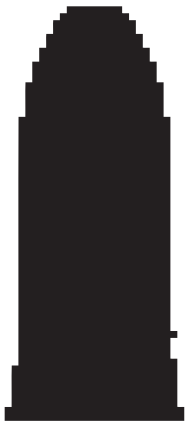

Figure 12. Solution computed on a mesh of 60×60 elements. The buckling constraint is set to $c_s = 0.5$ and the compliance constraint $c_{\max} = 5.5$. In this case, compared with Figure 11, the higher compliance constraint has led to a solution where this constraint is inactive and the buckling constraint is now active.

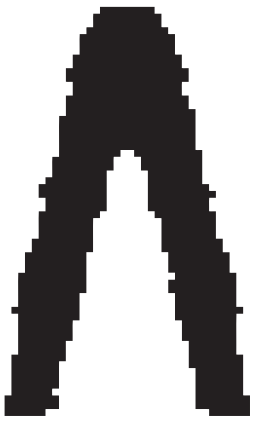

Figure 13. Solution computed on a mesh of 60×60 elements. The buckling constraint is set to $c_s = 0.4$ and the compliance constraint $c_{\max} = 8$. A volume of 0.276 is attained.

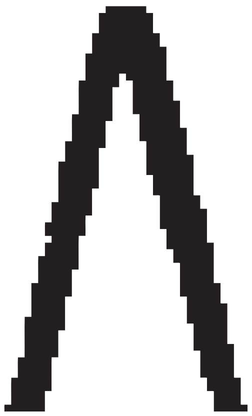

Figure 14. Solution computed on a mesh of 60×60 elements. The buckling constraint is set to $c_s = 0.1$ and the compliance constraint $c_{\max} = 8$. A volume of 0.183 is attained.

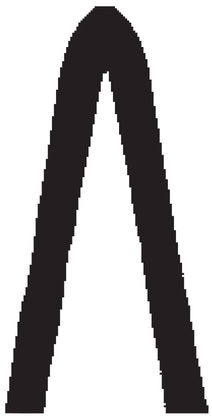

Figure 15. Solution computed on a mesh of 200×200 elements. The buckling constraint is set to $c_s = 0.1$ and the compliance constraint $c_{\max} = 8$. A volume of 0.1886 is attained. Compare with Figure 14.

From Figures 11–15, we see that the symmetry of the problem is not present in the computed solution. As Stolpe [30] and Rozvany [31] have shown, because we do not have continuous variables, we do not necessarily expect the optimal solution to these binary programming problems to be symmetric. The asymmetry in the computed solutions arise from (12) and (13) as only a subset of elements with precisely the same sensitivity values may be chosen to be updated and so the symmetry may be lost.

Table I summarizes the results obtained when solving the problem considered in Figures 14 and 15, but with varying mesh sizes. Note the problem size that the fast binary method has been able to solve. A computation on a two-dimensional mesh of 3×10^4 elements took less than 8 h on a modest desktop and 4×10^4 elements took around 12 h. This speed is attained because the number of derivative calculations appears to be not dependent on the number of variables. Figure 16 shows a log–log plot of the number of optimization variables against the wall-clock time taken to compute a solution. As the plot appears to have a gradient close to 2, this indicates that the time to compute a solution is $\mathcal{O}(n^2)$.

A detailed examination of the computational cost indicates that the vast majority of the computational cost is in the computation of the derivative of the buckling constraint (see the final column of Table I). A massively parallel implementation of this step is possible, and it is anticipated

Table I. Table of results for the centrally loaded column.

Problem size n	Objective	Derivative calculations	Analyses	Time (min) to 3 s.f.	Proportion of time on $\partial c_2/\partial x$
$30 \times 30 = 900$	0.266	11	26	0000.421	0.623
$40 \times 40 = 1600$	0.229	12	22	0001.100	0.782
$50 \times 50 = 2500$	0.213	11	21	0002.290	0.857
$60 \times 60 = 3600$	0.183	26	31	0006.730	0.901
$70 \times 70 = 4900$	0.187	24	28	0011.600	0.931
$80 \times 80 = 6400$	0.185	21	24	0018.100	0.948
$90 \times 90 = 8100$	0.184	20	22	0028.500	0.948
$100 \times 100 = 10000$	0.184	18	23	0040.600	0.966
$110 \times 110 = 12100$	0.188	19	21	0061.200	0.973
$120 \times 120 = 14400$	0.187	18	20	0084.500	0.978
$130 \times 130 = 16900$	0.184	19	23	0119.000	0.980
$140 \times 140 = 19600$	0.188	17	18	0154.000	0.984
$175 \times 175 = 30625$	0.173	20	22	0386.000	0.985
$180 \times 180 = 32400$	0.191	20	23	0458.000	0.989
$200 \times 200 = 40000$	0.188	21	24	0734.000	0.990
$317 \times 317 = 100489$	0.181	19	20	4230.000	0.996

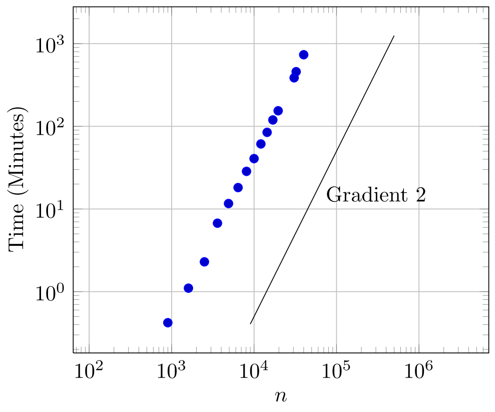

Figure 16. Log–log plot of time against the number of optimization variables. The gradient of this plot appears to be 2, suggesting that the time to compute the solution to a problem with n variables is $O(n^2)$.

that it should achieve near optimal speedup as no information transfer is required for the calculation of the derivative with respect to the individual variables.

5. CONCLUSIONS

The main computational cost associated with topology optimization involving buckling is the calculation of the derivatives of the buckling load. We have employed an analytic formula for this, but it still remains the most expensive part of the algorithm. To reduce the computational cost, we have developed an algorithm that aims to minimize the number of these computations that are required. The method is a descent method that enforces feasibility at each step and thus could be terminated early and would still result in a feasible structure.

We have numerically shown that the algorithm scales quadratically with the number of elements in the finite-element mesh of the design space. This corresponds to the analytical result that the derivative of the stress-stiffness matrix with respect to each of the design variables is an $\mathcal{O}(n^2)$ operation. The numerical experiments demonstrate the efficiency of the method for binary topology optimization using compliance and buckling constraints.

ACKNOWLEDGEMENTS

This paper was funded by the EPSRC with contract grant no. EP/E053351/1 and CASE award MCA 09 - 2008/2009.

REFERENCES

1. Wolsey L. *Integer programming*, Wiley-Interscience series in discrete mathematics and optimization. Wiley: New York, USA, 1998. Available from: http://books.google.com/books?id=x7RvQgAACAAJ
2. Arora J, Huang M. Methods for optimization of nonlinear problems with discrete variables: a review. *Structural Optimization* 1994; **8**:69–85.
3. Toakley A, Optimum design using available sections. *Journal of the Structural Division: proceedings of the American Society of Civil Engineers* 1968; **94**:1219–1241.
4. Stolpe M, Bendsøe MP. Global optima for the Zhou–Rozvany problem. *Structural and Multidisciplinary Optimization* 2010; **43**(2):151–164.
5. Farkas J, Szabo L. Optimum design of beams and frames of welded I-sections by means of backtrack programming. *Acta Technica Academiae Scientiarum Hungaricae* 1980; **91**(1):121–135.
6. John K, Ramakrishna C, Sharma K. Optimum design of trusses from available sections—use of sequential linear programming with branch and bound algorithm. *Engineering Optimization* 1988; **13**(2):119–145.
7. Sandgren E. Nonlinear integer and discrete programming for topological decision making in engineering design. *Journal of Mechanical Design* 1990; **112**(1):118–122. DOI: 10.1115/1.2912568. Available from: http://link.aip.org/link/?JMD/112/118/1
8. Sandgren E. Nonlinear integer and discrete programming in mechanical design optimization. *Journal of Mechanical Design* 1990; **112**(2):223–229. DOI: 10.1115/1.2912596. Available from: http://link.aip.org/link/?JMD/112/223/1.
9. Salajegheh E, Vanderplaats G. Optimum design of trusses with discrete sizing and shape variables. *Structural Optimization* 1993; **6**:79–85.
10. Beckers M. Dual methods for discrete structural optimization problems. *International Journal for Numerical Methods in Engineering* 2000; **48**(12):1761–1784.
11. Stolpe M, Svanberg K. Modelling topology optimization problems as linear mixed $\mathbf{0}--\mathbf{1}$ programs. *International Journal for Numerical Methods in Engineering* June 2003; **57**(5):723–739. DOI: 10.1002/nme.700. Available from: http://doi.wiley.com/10.1002/nme.700.
12. Achtziger W, Stolpe M. Truss topology optimization with discrete design variables—guaranteed global optimality and benchmark examples. *Structural and Multidisciplinary Optimization* December 2007; **34**(1): 1–20. DOI: 10.1007/s00158-006-0074-2. Available from: http://www.springerlink.com/index/10.1007/s00158-006-0074-2.
13. Achtziger W, Stolpe M. Global optimization of truss topology with discrete bar areas—Part I: theory of relaxed problems. *Computational Optimization and Applications* November 2008; **40**(2):247–280. DOI: 10.1007/s10589-007-9138-5. Available from: http://www.springerlink.com/index/10.1007/s10589-007-9138-5.
14. Achtziger W, Stolpe M. Global optimization of truss topology with discrete bar areas—Part II: implementation and numerical results. *Computational Optimization and Applications* 2009; **44**(2):315–341. DOI: 10.1007/s10589-007-9152-7.
15. Svanberg K. The method of moving asymptotes—a new method for structural optimization. *International Journal For Numerical Methods in Engineering* 1987; **24**:359–373.
16. Bendsøe MP, Sigmund O. *Topology Optimization: Theory, Methods and Applications*. Springer: Berlin, Germany, 2003.
17. Kočvara M. On the modelling and solving of the truss design problem with global stability constraints. *Structural and Multidisciplinary Optimization* April 2002; **23**(3):189–203. DOI: 10.1007/s00158-002-0177-3. Available from: http://www.springerlink.com/openurl.asp?genre=article&amp;id=doi:10.1007/s00158-002-0177-3
18. Kočvara M, Stingl M. Solving nonconvex SDP problems of structural optimization with stability control. *Optimization Methods and Software* October 2004; **19**(5):595–609. DOI: 10.1080/10556780410001682844. Available from: http://www.informaworld.com/openurl?genre=article&amp;doi=10.1080/10556780410001682844&amp;magic=crossref||D404A21C5BB053405B1A640AFFD44AE3
19. Bogani C, Kočvara M, Stingl M. A new approach to the solution of the VTS problem with vibration and buckling constraints. *8th World Congress on Structural and Multidisciplinary Optimization*, Lisbon, Portugal, 2009; 1–10.
20. Tenek LH, Hagiwara I. Eigenfrequency maximization of plates by optimization of topology using homogenization and mathematical programming. *JSME International Journal Series C* 1994; **37**(4):667–677.
21. Pedersen N. Maximization of eigenvalues using topology optimization. *Structural and Multidisciplinary Optimization* 2000; **20**(1):2–11.
22. Neves MM, Sigmund O, Bendsøe MP. Topology optimization of periodic microstructures with a penalization of highly localized buckling modes. *International Journal for Numerical Methods in Engineering* June 2002; **54**(6):809–834. DOI: 10.1002/nme.449. Available from: http://doi.wiley.com/10.1002/nme.449
23. Hunt G, Thompson J. *A General Theory of Elastic Stability*. Wiley-Interscience: London, UK, 1973.
24. Cook RD, Malkus DS, Plesha M. *Concepts and Applications of Finite Element Analysis*. John Wiley and Sons: London, UK, 1989.

25. HSL(2011). A collection of Fortran codes for large scale scientific computation. Available from: http://www.hsl.rl.ac.uk
26. Hogg J, Reid J, Scott J. Design of a multicore sparse cholesky factorization using DAGs. *SISC* 2010; **32**:3627–3649.
27. Ovtchinnkov E, Reid J. A preconditioned block conjugate gradient algorithm for computing extreme eigenpairs of symmetric and Hermitian problems. *Technical Report RAL-TR-2010-019*, STFC Rutherford Appleton Laboratory, Didcot, UK, 2010.
28. Huang X, Xie YM. *Evolutionary Topology Optimization of Continuum Structures*. John Wiley & Sons Ltd: Chichester, UK, 2010.
29. Williams J. Algorithm 232: heapsort. *Communications of the ACM* 1964; **7**(6):347–348.
30. Stolpe M. On some fundamental properties of structural topology optimization problems. *Structural and Multidisciplinary Optimization* 2010; **41**(5):661–670.
31. Rozvany GIN. Authors reply to a discussion by Gengdong Cheng and Xiaofeng Liu of the review article On symmetry and non-uniqueness in exact topology optimizationİ by George I. N. Rozvany (2011, Struct Multidisc Optim 43: 297317). *Structural and Multidisciplinary Optimization* September 2011; **44**(5): 719–721. DOI: 10.1007/s00158-011-0703-2. Available from: http://www.springerlink.com/index/10.1007/s00158-011-0703-2